Jour. Fac. Sci., Hokkaido Univ., Ser. VII (Geophysics), Vol. 7, No. 1, 47–57, 1981

The Horizontal Movement Speed of Cumulus Clouds in a Shear Flow: A Two-Dimensional Numerical Experiment

Hisashi Kon

Department of Geophysics, Faculty of Science
Hokkaido University, Sapporo 060, Japan

(Received October 30, 1980)

Abstract

Cumulus clouds in a shear flow are simulated by a two-dimensional slab-symmetric model with two different finite-difference schemes.

It is known that the horizontal speed of the top of simulated clouds is less than the ambient wind speed at that height. This is explained in the developing stage by the transformation of the circulation pattern arising from vertical wind shear and in the dissipating stage by the asymmetrical distribution of liquid water content arising from the transformation of circulation.

1. Introduction

The behavior of cumulus clouds in a shear flow is important for cloud dynamics. The effect has been studied by many researchers. In two-dimensional numerical experiments, Asai (1964) studied the behavior of cumulus convection in vertical shear flows. He obtained results in which he showed that the axis of the convection cell tilted down wind with height and that a vertical wind shear tended to suppress the development of the convection. Lipps (1971) and Wilkins et al. (1977) showed that dry thermal convections were also suppressed by vertical wind shear when convective rolls were transverse to the mean current. By a three-dimensional numerical experiment, Pastushkov (1975) and Cotton and Tripoli (1978) showed that a vertical wind shear did not always suppress the cumulus convection based on the energy transformation and the height of the cloud top, respectively. However they failed to pay attention to the horizontal movement of cumulus clouds. Recently, a wind field has been determined by the movement of clouds observed from Weather Satellites. Thus the difference between cloud and wind speeds should be known. It was discussed by Fujita and Pearl (1975) and Hasler et al. (1977).

Cumulus humilis clouds were observed by a stereophotogrammetric method and the difference of horizontal speeds between cloud and environment was discussed by Chiyu et al. (1973). Aspliden et al. (1978) indicated that tropical cumulus clouds moved slower than the current in which they were embedded.

In this paper, cumulus clouds will be simulated in a two-dimensional slab-symmetrical model with a vertical wind shear. Thus it was noted that the horizontal speed of cumulus cloud tops is slower than the ambient one.

2. Processes of numerical experiments

The basic equations used in the numerical experiment are the same as those used by Ogura (1963) except that the equations are converted from cylindrical to rectangular Cartesian coodinates to represent a general wind effect in the X-Z plane. The approximate saturation technic used by Ogura is also adopted as it is considered that the value of liquid water content is not so important.

Two finite-difference schemes are accepted to determine whether the difference produces a sharp distinction in the results. One will be called the A-series and the other will be referred to as B-series hereinafter. In both series, the reference pressure, the reference temperature and the surface wind speed are set at 1000 mb, 300 K and zero, respectively. And a positive linear vertical wind shear is adopted.

2.1 A-series

The domain concerned is confined to the rectangular atmospheric layer with a depth of 1.7 km and width of 6 km. The domain is divided into 100 m grid squares and a 10 sec time increment is adopted to calculate a set of finite-difference equations into which a set of differential equations is transformed. Advective terms in these equations are transformed into upstream-N difference scheme (Molenkamp, 1968). The forward time difference is used for the time derivative. As implicit diffusion is large in this scheme, diffusion terms are neglected. The centered difference is used for other terms. The initial perturbation which produces the convective motion is given as follows:

$$\Delta\theta_0 = \Delta\theta \cdot \exp\{-9\times10^{-6}\times(X-1500)^2\} \cdot \sin\{\pi\,(Z-100)/600\}\,,$$

$$0 \leqq Z \leqq 700_m\,.$$

A boundary condition used by Takeda (1971) was adopted. Six cases are

Table 1. Parameters used in the each case study.

case	$\Delta\theta$(°C)	du/dz (sec^{-1})	H (m)	Γ (°C/100m)
A1	1.0	0	1200	0.64
2	1.2	0.0025	1200	0.64
3	1.0	0.005	1200	0.64
4	1.2	0.01	1200	0.64
5	1.2	0.01	1200	0.98
6	1.0	0.0025	700	0.64
B1	1.5	0	1400	0.64
2	1.5	0.005	1400	0.64

$\Delta\theta$: the maximum temperature excess of trigger, du/dz: strength of wind shear, H: inversion height and Γ: temperature lapse rate.

dealt with in this series. The initial conditions are as listed in Table 1. As the purpose of this paper is to examine the horizontal speed of cumulus clouds, the vertical wind shear is varied to four stages and a large relative humidity is used to readily produce a cloud. The humidity is 95% in the layer lower than 1200 m in height and above the level it is linearly decreased at a rate of 18% to 100 m. The temperature lapse rate is –0.64 degree/100 m (except for case A5 which is –0.98 degree/100 m) in the lower layer and there is an inversion of 1.6 degree/100 m above the level. Case A6 is the same as case A2 except that the inversion height is lowered to 700 m and $\Delta\theta$ is 1.0 degree.

2.2 *B-series*

The domain is confined to a 2.5 km depth and 4 km width as shown in Fig. 1. Cyclic boundary conditions are adopted in the lateral boundary. Advective terms in basic equations are transformed to flux form and a finite-difference scheme and the staggered grid arrangements showed by Kimura (1975) are

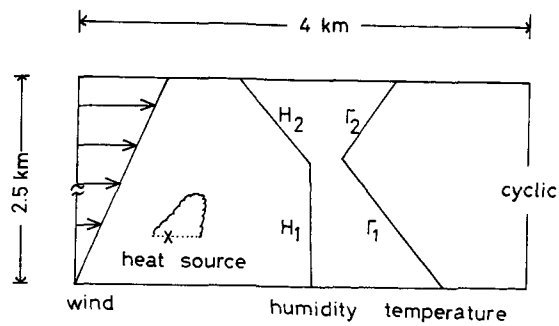

Fig. 1. Schematic representation of initial condition used in B-series.

used. The time integration is performed with the centered scheme but the Euler-Backward scheme is used in every 11 times. The interval of time increment is changed from 5 sec for B1 and to 2 for B2 to stabilize the solution. The trigger is given by following formula:

$$\Delta\theta_0 = \Delta\theta \exp\{-6\times10^{-7}\times(X-1900)^2\}\cdot\sin\{\pi(Z-300)/600\}\,,$$
$$300 \leqq Z \leqq 900_m\,.$$

The temperature lapse rate is the same with A-series except that the height of inversion is 1400 m. Relative humidity is 95% in the lower layer and it is decreased at a rate of 6% to 100 m above 1400 m. A constant eddy diffusion coefficient (50 m^2/s) is adopted in diffusion terms. Two cases are dealt with in this series (Table 1).

The finite-difference scheme in B-series is complicated, however the variables are more conservative than A-series. The scheme in B-series generates an instability of calculation after a certain time has elapsed. On the other hand, although the scheme used in A-series has a large implicit diffusion, it is the simplest one and stabilizes the solutions. Accordingly six results are obtained by A-series.

3. Results

Simulated clouds in case A2 are shown at 5, 10, 15 and 20 min of elapsed time in Fig. 2. It is seen in the figure that the cloud is carried downwards, being inclined by a vertical wind shear and that the height of cloud base is very low due to the large humidity. The cloud is grown by buoyancy initially supplied and by the energy of the conditionally unstable layer. At 20 min, a vertical development is suppressed by a stable layer aloft and reaches the maximum cloud size. The lowest part of the cloud is beginning to dissipate. Solid lines and chain lines show the isopleth of liquid water content and maximum liquid water content, respectively, in Fig. 2. The horizontal speed of the cloud base and the top is measured by the displacement of the position of the maximum liquid water content in successive times. That is to say, the speed of the position is calculated by means of dividing the distance shown by arrows in Fig. 2 by the required times. The ratio of the cloud speed to the ambient wind speed at that height is shown by γ. It is noted that the values are smaller than unity at the cloud top and larger than unity at the cloud base. In this numerical experiment, the height of the cloud base is very low because the relative humidity of the lower layer is 95%. Therefore

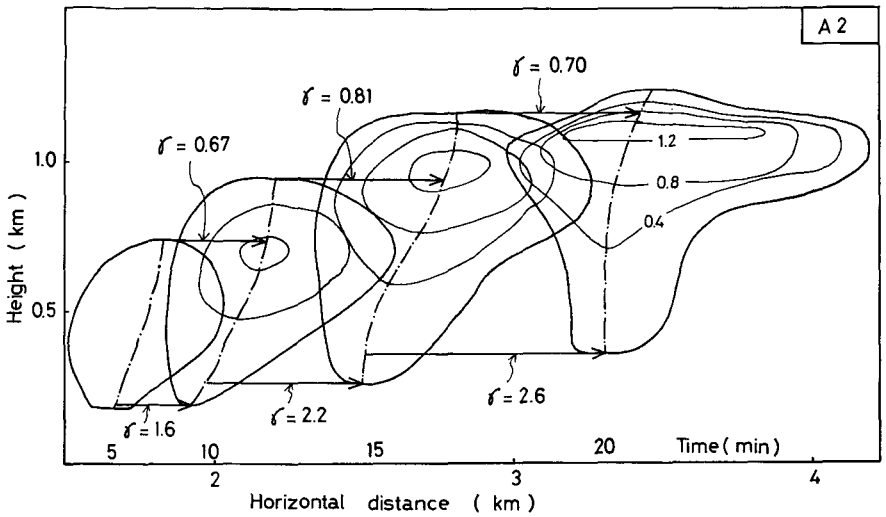

Fig. 2. Cloud development in case A2 at 5, 10, 15 and 20 min. Solid lines and chain lines indicate the isopleth of liquid water content and maximum liquid water content, respectively. γ is the ratio of cloud speed to ambient wind speed. The elapsed time is shown in the lower part.

when a comparison with an observation is attempted, application of the cloud top value is reasonable.

Cloud and stream function deviation from the initial basic state in case A2 are shown in Fig. 3 at 10 min of the elapsed time. It is seen that the updraft is dominant in the front of the cloud base and to the rear of the cloud top. This pattern of updraft indicates that the cloud is developed in front of the cloud base and to the rear of the cloud top. Accordingly, the cloud base appears to move faster and the cloud top to move slower than the ambient wind speed at that height. If the updraft completely adopted itself to the surrounding flows, the axis of the updraft in the cloud would become parallel to the vertical profile of the ambient wind speed. The discrepancy between the axes of updraft and vertical profile of ambient wind speed may be explained by the vertical transport of horizontal momentum.

Fig. 4 shows a cloud and a stream function deviation on case A3 at 10 min. The cloud becomes smaller because of suppression by a strong shear. The pattern of stream line is almost the same as in case A2.

In case A6, the inversion layer is lowered to 700 m height. As the development of the cloud is then suppressed, the process from the initial

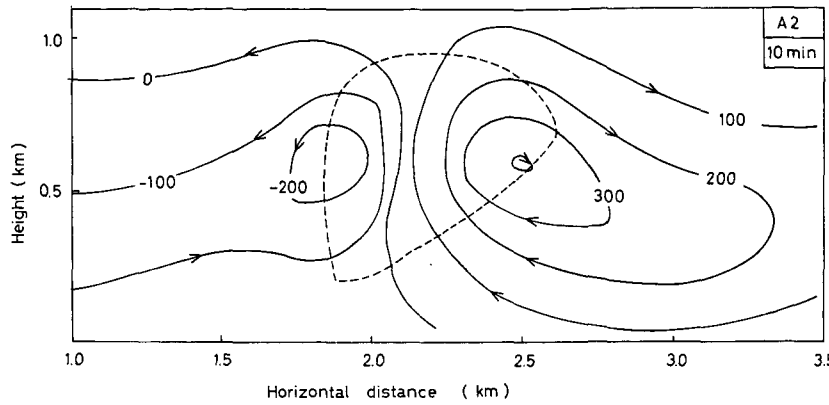

Fig. 3. The stream function deviation (m^2/s) from initial basic state in case A2 at 10 min. Cloud region outlined by dashed line.

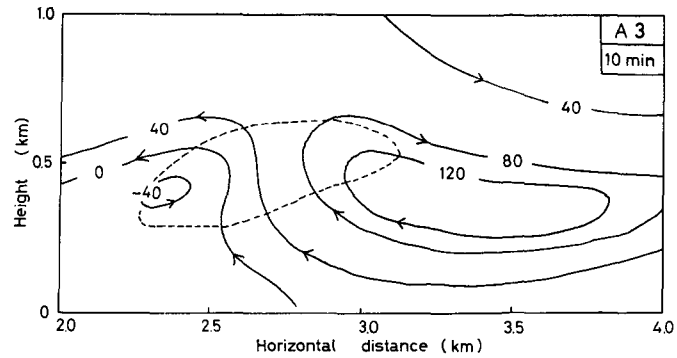

Fig. 4. As in Fig. 3 except in case A3.

state to the dissipating stage of the cloud is seen in Fig. 5. In the dissipating stage, it is noted in the figure that the rear part of the cloud remains because of the asymmetrical distribution of liquid water content owing to the transformation of a circulation pattern as shown in Figs. 3 and 4. Accordingly the horizontal speed of the cloud becomes slower than the ambient wind speed.

Fig. 6 shows the simulated cloud on case B2. As the inversion layer is higher than A-series, the cloud can penetrate to higher levels. The cloud axis shown by the maximum liquid water content inclines to the lee and γ

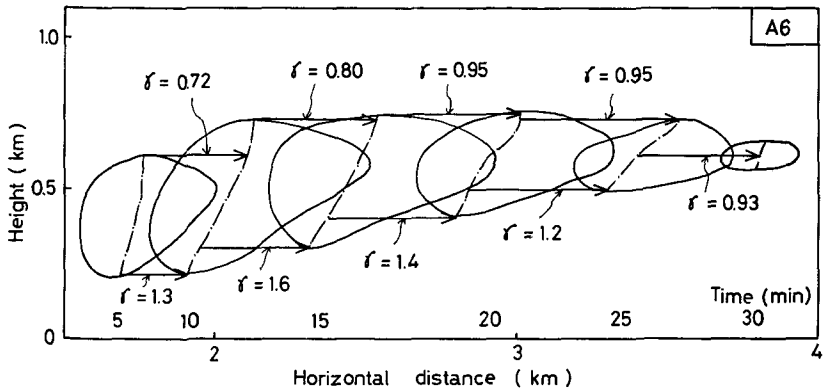

Fig. 5. As in Fig. 2 except in case A6.

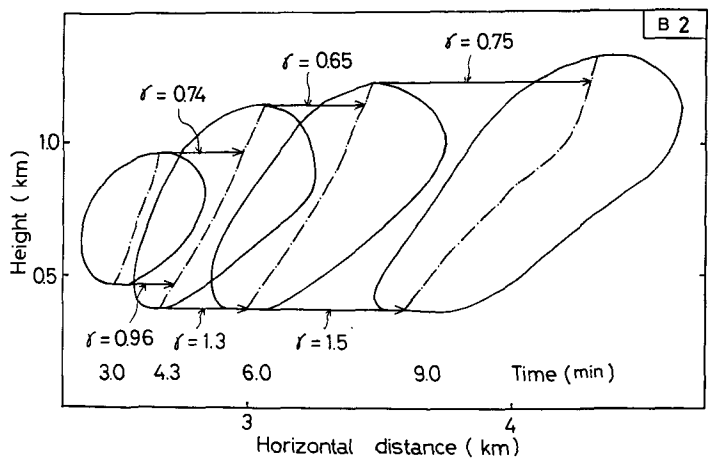

Fig. 6. As in Fig. 2 except in case B2.

is smaller than unity in the cloud top and larger than unity in the cloud base as well as A-series.

Fig. 7 shows the distribution of vertical speed (solid lines) and horizontal speed deviation (dashed lines). Updraft regions are extended in front of the cloud base and to the rear part of the cloud top. This indicates that the axes of updraft and cloud are shifted.

Ratio γ of the horizontal speed of the cloud top to the ambient wind speed, the maximum cloud size and the maximum upward speed are summarized in

Table 2. The value of γ is exactly unity in case B1 and is nearly unity in case A1. The ratio is smaller than unity in cases with a vertical wind shear. The inhibiting effect of a wind shear on the development of a cumulus cloud is noted from the fact that case A3 and A4 have a small cloud size comparing with case A1 and A2, respectively. The cloud growth of case A5 is stronger than case A4 because of a large temperature lapse rate in the lower layer. And it is seen that the cloud size depends on the maximum upward speed under the same temperature lapse rate (A1, A2, A3 and A4).

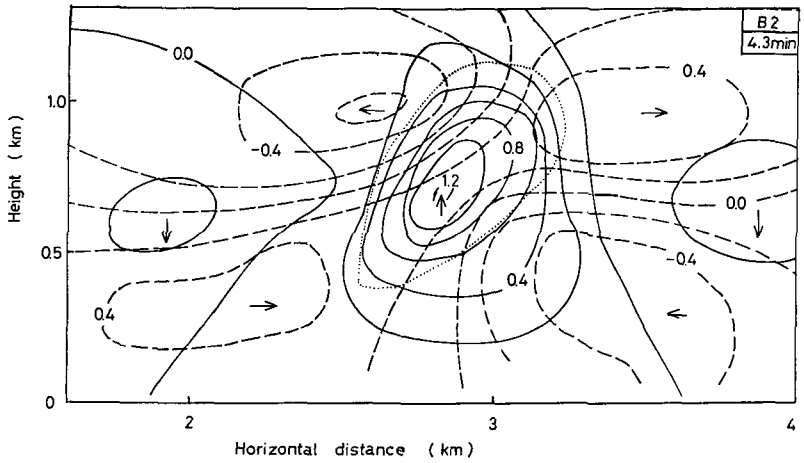

Fig. 7. The distribution of vertical speed and horizontal speed deviation in case B2 at 4.3 min. Cloud region outlined by dotted line.

Table 2. Summary of results obtained by numerical experiments.

case	size ($\times 10^3$m^2)	γ_{top}	W_{max} (m/s)
A1	300	0.97	1.46
2	570	0.67~0.81	2.32
3	200	0.84~0.89	0.26
4	90	0.90~0.93	0.13
5	580	0.70	0.92
6	210	0.72~0.95	*
B1	510**	1.0	2.32
2	610	0.65~0.75	1.87

* The datum was not printed out.

** The calculation was stopped before the cloud reached the maximum cloud size.

4. Comparison with an observation

In a previous paper (Kon, 1981), the difference between horizontal speed of observed cumulus clouds and ambient wind speed was discussed. The results obtained by the present numerical experiment will be compared with

Table 3. Points for comparison with an observation.

case	time (min)	Δu (m/s)	z (m)	u_c (m/s)	R (m)
A2–1	5–10	0.70	730	1.13	310
2	10–15	0.60	970	1.83	410
3	15–20	0.87	1160	2.03	530
A3–1	5–10	0.60	580	2.30	300
2	10–15	0.80	680	2.60	370
3	15–20	0.73	680	2.67	350
A4	5–10	0.93	560	4.67	150
A5	5–10	1.60	680	5.20	400
A6–1	5–10	0.62	670	1.11	280
2	10–15	0.72	730	1.37	340
3	15–20	0.53	740	1.57	320
4	20–25	0.38	740	1.73	280
B2–1	3–4.3	1.05	960	3.75	250
2	4.3–6	1.75	1150	4.00	290
3	6–9	1.54	1230	4.61	340

Δu: difference between horizontal wind and cloud speeds, z: cloud top height, u_c: horizontal cloud speed and R: radius of cloud.

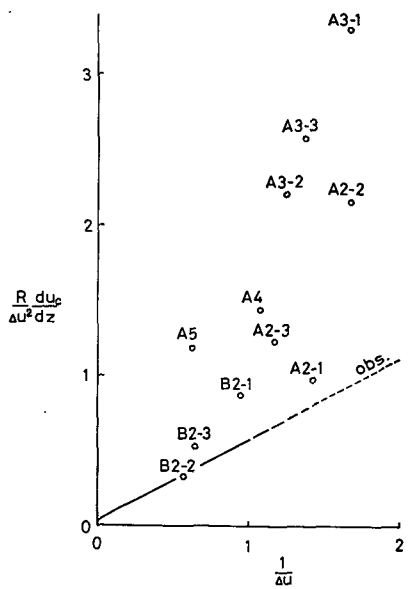

Fig. 8. Comparison with an observation (see in Fig. 1 by Kon, 1981). The front number and the end number of a point show each case study and the order of the time elapsed, respectively.

the results of the previous paper. The cloud top height: z, the maximum cloud radius: R and the difference between both speeds: Δu at the cloud top for each case are shown in Table 3. The average value of successive two clouds as seen in Fig. 2 is adopted for z and R. For comparison with the observation, $1/\Delta u$ and $R/\Delta u^2 \times du_c/dz$ are calculated by formula (7) of the previous paper. The results are plotted in Fig. 8. The front numbers which are entered on the points in the figure show each case study and the rear numbers show the order of the cloud life. The solid line is the best fit line obtained for the observation. The results of the numerical experiments are dispersed because Δu is too small. The points of A-series were widely distributed in the upper part of the best fit line. First, it was considered that this was caused by the large implicit diffusion of the finite-difference scheme of A-series. Secondly, it was considered that the compensating downdraft in the slab-symmetric model is large and spreads in space widely (Soong and Ogura, 1973) and the influence largely acts for this two-dimensional model. Further as the cloud top is low, the effect was promoted. On the other hand, the points of B-series are found near the line as a reflection of a detailed numerical scheme and a deep convective layer.

5. Conclusion

An effect of vertical wind shear on a cumulus cloud which is considered in a two-dimensional slab-symmetric model is studied by numerically integrating an appropriate set of equations. And the difference between wind and cloud speeds is discussed.

The horizontal speed of the top of simulated clouds is less than that of the ambient wind speed at that height. It is explained by a transformation of a circulation pattern due to the vertical shear field. That is to say, the upward flow is active to the rear of the cumulus cloud. And the transformation makes an asymmetrical distribution of liquid water content. That is to say, the maximum liquid water content is generated in the rear side of the cloud. Accordingly the movement speed of the cloud appears to be less than the ambient wind speed in the dissipating stage. It is noted that the difference between the horizontal speed of the clouds and ambient winds depends on the vertical speed within the cloud. When the results of the numerical experiments are compared with an actual observation of cumulus clouds, it is noted that B-series which has a detail finite-difference scheme and a deep convective layer is more realistic than A-series. The horizontal speed of

the cloud base is faster than the ambient wind speed in these numerical experiments. It is explained by an inflow in front of the cloud base.

Acknowledgements

The author wishes the express his hearty thank to Prof. C. Magono for his encouraging discussions and Prof. K. Kikuchi for his encouragement throughout this work. Thanks are extended to Dr. T. Chiyu for his help in carrying out the research.

References

Asai, T., 1964. Cumulus convection in the atmosphere with vertical wind shear, J. Meteor. Soc. Japan, **42**, 245–259.

Aspliden, C.I., R.S. Hipskind, J.B. Sabine, P. Valkenaar and R.L. DeSouza, 1978. Three-dimensional wind structure around convective elements over a tropical island, Tellus, **30**, 252–259.

Chiyu, T., H. Kon and C. Magono, 1973. The moving velocity of cumulus humilis clouds, J. Meteor. Soc. Japan, **51**, 43–53.

Cotton, W.R. and G.J. Tripoli, 1978. Cumulus convection in shear flow-Three-dimensional numerical experiments, J. Atmos. Sci., **35**, 1503–1521.

Fujita, T.T. and E.W. Pearl, 1975. Satellite-tracked cumulus velocities, J. Appl. Meteor., **14**, 407–413.

Hasler, A.F., W.E. Shenk and W.C. Skillman, 1977. Wind estimates from cloud motions: Results from phase I, II and III of an insitu aircraft verification experiment, J. Appl. Meteor., **16**, 812–815.

Kimura, R., 1975. Dynamics of steady convections over heat and cool islands, J. Meteor. Soc. Japan, **53**, 440–457.

Kon, H., 1981. A determination of entrainment rate and drag coefficient of cumulus cloud, J. Fac. Sci., Hokkaido Univ. Ser. VII, **7**, 41–46.

Lipps, F.B., 1971. Two-dimensional numerical experiments in thermal convection with vertical shear, J. Atmos. Sci., **28**, 3–19.

Molenkamp, C.R., 1968. Accuracy of finite-difference methods applied to the advection equation, J. Appl. Meteor., **7**, 160–167.

Ogura, Y., 1963. The evolution of a moist convection element in a shallow conditionally unstable atmosphere: A numerical calculation, J. Atmos. Sci., **20**, 407–424.

Pastushkov, R.S., 1975. The effects of vertical wind shear on the evolution of convective clouds, Quart. J. Roy. Meteor. Soc., **101**, 281–291.

Soong, S.T. and Y. Ogura, 1973. A comparison between axi-symmetric and slab-symmetric cumulus cloud models, J. Atmos. Sci., **30**, 879–893.

Takeda, T., 1971. Numerical simulation of a precipitating convective cloud: the formation of a "long-lasting" cloud, J. Atmos. Sci., **28**, 350–376.

Wilkins, E.M., Y.M. Sasaki and H.L. Johnson, 1977. Interactions between a discrete convective element and a shearing environment: a numerical simulation, Mon. Wea. Rev., **105**, 261–269.